AIP Journal of Applied Physics

Photoluminescence, deep level transient spectroscopy and transmission electron microscopy measurements on MeV self-ion implanted and annealed n-type silicon

D. C. Schmidt, B. G. Svensson, M. Seibt, C. Jagadish, and G. Davies

Citation: Journal of Applied Physics **88**, 2309 (2000); doi: 10.1063/1.1288020
View online: http://dx.doi.org/10.1063/1.1288020
View Table of Contents: http://scitation.aip.org/content/aip/journal/jap/88/5?ver=pdfcov
Published by the AIP Publishing

Articles you may be interested in

Energy level(s) of the dissociation product of the 1.014 eV photoluminescence copper center in n-type silicon determined by photoluminescence and deep-level transient spectroscopy
J. Appl. Phys. **114**, 033508 (2013); 10.1063/1.4813878

Transmission electron microscopy characterization of secondary defects created by MeV Si, Ge, and Sn implantation in silicon
J. Appl. Phys. **88**, 1312 (2000); 10.1063/1.373819

Effect of ion mass on the evolution of extended defects during annealing of MeV ion-implanted p-type Si
Appl. Phys. Lett. **74**, 1141 (1999); 10.1063/1.123468

Electrical characterization of the threshold fluence for extended defect formation in p -type silicon implanted with MeV Si ions
Appl. Phys. Lett. **72**, 3044 (1998); 10.1063/1.121535

Ion-beam annealing of electron traps in n -type Si by post- H + implantation
J. Appl. Phys. **82**, 1053 (1997); 10.1063/1.365870

AIP APL Photonics

APL Photonics is pleased to announce **Benjamin Eggleton** as its Editor-in-Chief

[This article is copyrighted as indicated in the article. Reuse of AIP content is subject to the terms at: http://scitation.aip.org/termsconditions. Downloaded to] IP: 130.56.107.12 On: Fri, 25 Sep 2015 02:34:00

Photoluminescence, deep level transient spectroscopy and transmission electron microscopy measurements on MeV self-ion implanted and annealed *n*-type silicon

D. C. Schmidt and B. G. Svensson
Royal Institute of Technology, Solid State Electronics, Electrum 229, S-16440 Kista-Stockholm, Sweden

M. Seibt
IV. Physikalisches Institut, Universität Göttingen, Bunsenstr. 13-15, D-37073 Göttingen, Germany

C. Jagadish
Department of Electronic Materials Engineering, Research School of Physical Sciences and Engineering, Australian National University, Canberra ACT 0200, Australia

G. Davies[a)]
Physics Department, King's College London, Strand, London WC2R 2LS, United Kingdom

(Received 28 February 2000; accepted for publication 8 June 2000)

Deep-level transient spectroscopy (DLTS), photoluminescence (PL), and transmission electron microscopy (TEM) measurements have been made on *n*-type silicon after implanting with 5.6 MeV Si^{3+} ions using doses of 10^9-10^{14} cm^{-2} and anneals at 525 and 750 °C. In all the samples, there is only a small dependence of the widths and energies of the PL zero-phonon lines on implantation dose, allowing the high resolution of PL to be exploited. In samples annealed at 525 °C, the PL intensity can provide a measure of the concentration of defects over the implantation range, 10^9-10^{12} cm^{-2}. Carbon-hydrogen complexes are identified as transient species with increasing dose, and the ''T'' center is related to a DLTS trap 0.20 eV below the conduction band energy E_c. At the highest doses in these samples, TEM imaging shows the presence of nanometer-sized clusters, and the PL spectra show that many previously unreported defects exist in the implanted zone, in addition to two broad bands centered on ~885 and ~930 MeV. The multiplicity of defects supports recent suggestions that a range of interstitial complexes is present in the annealed samples. Annealing at 750 °C produces complete recovery in both the DLTS and PL spectra for doses of less than 10^{13} cm^{-2}. At higher doses, {113} self-interstitial aggregates are observed in TEM, along with the ''903'' PL signal associated with the {113} defects, and the $E_c-0.33$ eV ''KA'' DLTS trap. These data support the recent identification of that trap with the {113} defects. The well-resolved PL spectra show that many previously reported defects also exist in samples implanted with a dose of 10^{14} cm^{-2} and annealed at 750 °C, again implying the presence of a range of interstitial complexes. © *2000 American Institute of Physics.* [S0021-8979(00)00218-8]

I. INTRODUCTION

Ion implantation is a crucially important tool in the manufacture of silicon semiconductor devices as a result of its ability to introduce controlled quantities of dopants with high spatial precision. In addition to introducing the dopant, the implantation process produces radiation damage defects, and necessarily introduces one extra atom per dopant atom into the crystal. During implants at room temperature, the generated vacancies and self-interstitials are highly mobile, and in addition to recombining and clustering, they may create a large variety of defects through complexing with impurities.[1] Annealing the damage then becomes an important part of the implantation strategy; the annealing procedures used must heal the silicon while avoiding thermal- and transient-enhanced diffusion. Simulation software used to predict the properties of implanted and annealed silicon requires an accurate understanding of the distribution of the implanted dopant species, which can be obtained, e.g., from secondary ion mass spectrometry measurements. However, it is also necessary to identify the chemistry and molecular structure of the defects that exist at each stage.[2]

Recently, a widely used defect characterization technique has been deep level transient spectroscopy (DLTS). For example, after annealing above 400 °C many defect levels have been detected by DLTS in *n*-type silicon following implantations using doses as low as 1×10^8 cm^{-2} and up to 5×10^{13} cm^{-2}.[3] These defects were tentatively considered to be of interstitial nature, partially based on the fact that they have previously been observed following implantations with many different ions (protons,[4,5] alpha particles,[5] germanium,[6,7] and SiH^{++}[8]). DLTS has also identified the threshold dose for creating {113} self-interstitial aggregates at $\sim4\times10^{13}$ cm^{-2} Si ions in the MeV range.[9,10] In contrast, with very few exceptions,[11,12] photoluminescence (PL) has not recently been applied to ion-implanted samples even though there have been significant advances in the identifi-

[a)]Author to whom correspondence should be addressed; electronic mail: gordon.davies@kcl.ac.uk.

 © 2000 American Institute of Physics
[This article is copyrighted as indicated in the article. Reuse of AIP content is subject to the terms at: http://scitation.aip.org/termsconditions. Downloaded to] IP: 130.56.107.12 On: Fri, 25 Sep 2015 02:34:00

cation of PL centers. In this article we report on the PL from ion-implanted silicon, comparing the results with DLTS and transmission electron microscopy (TEM) measurements on similarly prepared samples.

In implantation studies there are many possible choices for the starting material, the species, energy and dose of the implant, and the annealing regimes. In this work we have implanted *n*-type Czochralski (Cz) silicon with 5.6 MeV Si^{3+} ions over the dose range of from 10^9 to 10^{14} cm^{-2}. Silicon ions have been implanted in order to limit the radiation-activated chemistry, by not introducing impurities. The energy of the implant results in an initial damage depth profile that peaks ~ 3.5 μm into the crystal, allowing the DLTS and PL measurements to be made in the implanted region (see Sec. II). We show in Sec. III A that there is only a small increase with dose of the widths of the PL lines, and negligible change in their energy, so that the lines can be used to characterize defects throughout the dose range. In Sec. III A we also show that the intensity of each PL line can be an approximate measure of the concentration of the related center up to doses of 10^{12} cm^{-2}. Two annealing temperatures have been used, 525 and 750 °C. A half hour at either temperature is sufficient to anneal the products of room-temperature damage at low doses.[1] In the samples used here, these unannealed products are created by the interactions of a vacancy with an oxygen atom to create the *A* center, with a phosphorus atom to give the *E* center, or with another vacancy to create a divacancy, while a self-interstitial may react with carbon or boron to produce mobile interstitial species. These defects are destroyed by 30 min anneals at 525 °C.[1] The higher anneal temperature of 750 °C is expected to remove centers seen by DLTS according to Benton *et al.*;[13] however, the same workers report a dose dependence in the thermal stability of the defects, and we will show that many previously unreported PL species continue to exist in our high-anneal implanted samples (see Sec. III B). This result is consistent with the conclusion from the modeling of defect clusters carried out recently by Cowern *et al.*;[14] namely, a range of ion-implantation clusters may persist after prolonged annealing. Annealing at the lower temperature (525 °C) will be shown to generate a large number of well-resolved PL lines (see Sec. III C). Two will be identified as carbon-hydrogen complexes, one of which will be firmly related to a DLTS feature. However, the great majority of the lines have unknown origins, and the high resolution spectra available here show that they cannot be related to simple point defects whose spectra are known from electron-radiation studies. We also show in Sec. III C that transmission electron microscopy establishes that nanometer-sized clusters can be created in samples annealed as low as 525 °C, in contrast to the literature.[12,13]

We begin by outlining the experimental techniques.

II. EXPERIMENTAL ASPECTS

Samples of *n*-type ⟨100⟩ Cz silicon of resistivity 6–8 Ω cm ($\sim 5-8\times10^{14}$ phosphorus cm^{-3}) were implanted with 5.6 MeV $^{28}Si^{3+}$ ions at room temperature with doses of 10^9 to 10^{14} cm^{-2} using the 1.7 MV NEC Tandem accelerator at the Australian National University. The maximum in the depth distribution of the incoming particles is expected at ~ 3.5 μm from the surface according to the stopping and range of ions in matter (SRIM)[15] (version 2000.38), and this depth was confirmed by TEM (see Secs. III B and III C). Before implantation, infrared absorption measurements established the concentrations of oxygen and carbon as $\sim 6\times10^{17}$ cm^{-3} and $<10^{16}$ cm^{-3}, respectively. Photoluminescence measurements allow all shallow dopants to be identified. Apart from phosphorus, the only other shallow center detectable before implantation was boron, at a concentration (determined using the method outlined for *P* in Sec. III B) of $[B]\sim 5\times10^{12}$ cm^{-3}.

The implanted samples were annealed for 30 min at 525 or 750 °C in a tubular oven under constant argon flow. Identically treated samples were used for the photoluminescence studies and for the transmission electron microscopy studies or were prepared for DLTS measurements by a standard cleaning process ending in rinsing in diluted HF, and depositing gold Schottky contacts by thermal evaporation at a base pressure of 2×10^{-6} Torr at nominal room temperature.

The DLTS system consisted of a 1 MHz capacitance bridge, a 50 MHz pulse generator, and a liquid nitrogen bath into which a Semilab sample holder is placed.[16] The setup, which correlates the DLTS signal with a lock-in weighting function, is able to collect nine rate windows simultaneously, which are used to determine the trap signatures via an Arrhenius plot. During a temperature scan from 77 to 300 K, eight rate windows from $(20\text{ ms})^{-1}$ to $(2.56\text{ s})^{-1}$ were simultaneously recorded. The steady state reverse bias for all measurements was chosen to be -10 V, while the filling pulse was 10 V. In this way the whole damage profile was covered, except for the zero bias depletion width, and the DLTS spectra approximate to a mean defect distribution through the implanted layer. The width of the filling pulse was chosen to be 10 ms to ensure that all traps, including those with small capture cross sections, were completely saturated. The levels will be labeled by their peak temperatures so that, e.g., a defect with an observed maximum at 210 K is the "*E*(210)" center.

Photoluminescence measurements were made using a Nicolet 60SX Fourier transform spectrometer fitted with a Ge diode detector for the spectral range 740–1180 meV and an InSb detector to extend the range down to 450 meV. PL centers will be labeled here by the energy of the zero-phonon line or of other very sharp structure. Samples were immersed in liquid helium for measurements at 4.2 K or were in a flow of helium gas for higher temperatures. Excitation was by a 514 nm argon laser operated at a constant power of about 400 mW. It will be shown in Sec. III A that the excitation is expected to be confined in the first few micrometers of the crystals. Both the DLTS and PL spectra are therefore sampling similar depths and are matched to the depth of the implant.

Cross-section TEM samples along [011] were prepared by mechanical thinning down to 10 μm followed by ion-beam milling using Ar ions at energies below 3.5 keV and incident angles below 12°. Electron micrographs were obtained at 200 kV in a Philips CM200-UT-FEG which has a

[This article is copyrighted as indicated in the article. Reuse of AIP content is subject to the terms at: http://scitation.aip.org/termsconditions. Downloaded to] IP: 130.56.107.12 On: Fri, 25 Sep 2015 02:34:00

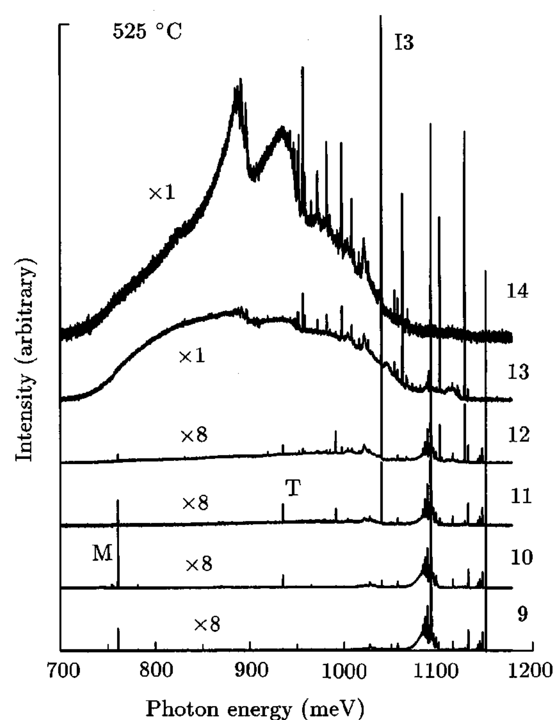

FIG. 1. An overview of the PL spectra at 4.2 K from samples implanted with doses from 10^9 cm^{-2} (labeled "9," bottom spectrum) to 10^{14} cm^{-2} (labeled "14," top spectrum) and annealed for 30 min at 525 °C. The strengths of representative sharp-line features are given in Fig. 3. PL at energies greater than 1030 meV in the 10^9 cm^{-2} spectrum (and replicated in the others) is produced by phosphorus, boron, free excitons and the electron-hole plasma and is not of fundamental interest here. For clarity the spectra are displaced vertically; the zero level is shown by the high energy end of each spectrum.

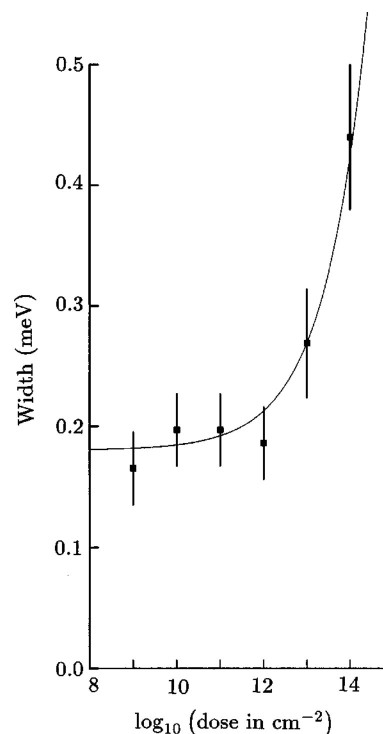

FIG. 2. The widths of the I3 zero-phonon line at 1039 meV, measured at 4.2 K, in samples implanted with doses from 10^9 to 10^{14} cm^{-2} and annealed for 30 min at 525 °C. The line represents an increase in width proportional to the square root of the implantation dose in addition to a zero-dose width of 0.18 meV.

point resolution of 0.187 nm. High-resolution images were taken near Scherzer focus under 9-beam conditions along the [011] zone axis orientation.

III. RESULTS AND DISCUSSION

A. Overview of the photoluminescence spectra

DLTS is well established as a defect probe of implanted silicon, but since PL has been little used it is important to establish the value and limits of the technique. (A general review of the use of PL in studying point defects in silicon is given in Ref. 17.) For PL to be successfully applied to ion-implanted material, the PL from point defects in the implanted region must be recognizable. As a measure of the degradation of the PL signals caused by the damage, we note that point defects in crystalline silicon typically produce PL bands whose zero-phonon lines have full widths at half height of $W \sim 0.1-0.2$ meV when measured at 4.2 K. The intrinsic resolution of the technique is therefore high, since W is about four orders of magnitude smaller than the energy gap of silicon. We will discuss the measured spectra in detail below, but we note that all of the samples annealed at 525 °C show the "I3" zero-phonon line at 1039 meV, produced by a radiation-damage defect (see Fig. 1). Figure 2 shows that the full width at half height of the I3 line increases from the value expected in Czochralski silicon, ~0.2 meV, but only by a factor of about 2 at the highest dose used here. The width of a zero-phonon line monitors the variation in strain over the ensemble of centers in the silicon, and the width is expected to increase in proportion to the concentration of the point defects, as is observed in electron-irradiated silicon (e.g., Fig. 81 of Ref. 17). Clearly, although the random strains are increasing, the line remains sufficiently sharp to be identifiable. The sublinear growth in width with dose is qualitatively consistent with the broadening being caused by the strain fields of defect aggregations in the more implanted samples.[18]

No other defect-induced zero-phonon line in the samples can be followed through a complete set of samples in this way, but all the zero-phonon lines are sufficiently sharp in all the samples that there is no difficulty in identifying them. (The only exceptions are broader features that are related to self-interstitial aggregates, as discussed in Sec. III B.) The peak energy of each line is also invariant to within ±0.03 meV in all the samples where it was observed. Thus, there is no significant degradation of the PL spectra by the implantation in the dose range used here.

The location of the sources of the PL cannot be determined directly from these data. The primary excitation of silicon using 514 nm Ar^+ laser light occurs with an exponential decay distance of 1 μm, and so is within the implantation depth of 3.5 μm. The electrons and holes, or excitons, created by the light diffuse through the crystal for a distance which critically depends on the impurity content. Photoluminescence has been detected over 100 μm from the excitation point in pure silicon,[19] decreasing to ~1 μm in epitaxial silicon with $\sim 10^{16}$ cm^{-3} dopant content.[20] In the present

[This article is copyrighted as indicated in the article. Reuse of AIP content is subject to the terms at: http://scitation.aip.org/termsconditions. Downloaded to] IP: 130.56.107.12 On: Fri, 25 Sep 2015 02:34:00

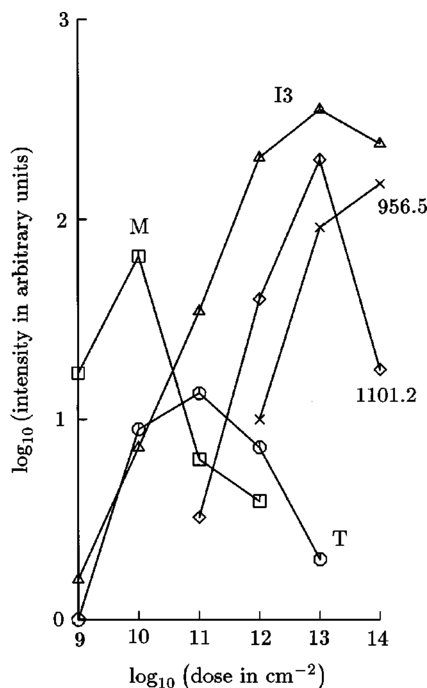

FIG. 3. Measured intensities (areas) of PL from representative sharp features (zero-phonon lines) in samples implanted with doses from 10^9 to 10^{14} cm^{-2} and annealed for 30 min at 525 °C. Datum points are shown, respectively, by squares and circles for the M and T lines, by triangles for the I3 line, and by diamonds and crosses for the 956.5 and 1101.2 meV lines. Note that both scales are logarithmic.

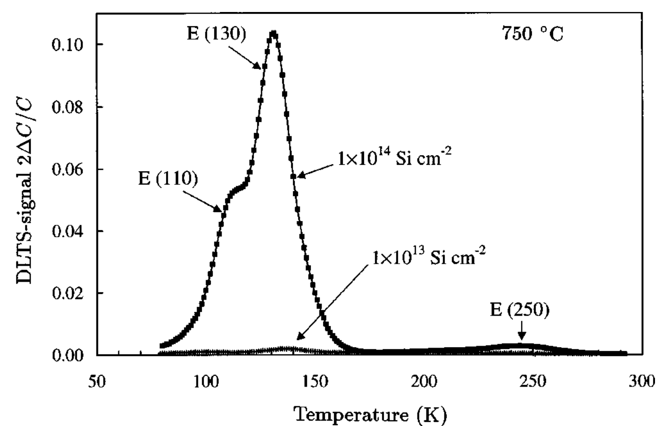

FIG. 4. DLTS spectra of the samples implanted with doses of 10^{13} and 10^{14} cm^{-2} following a 30 min anneal at 750 °C. The reverse bias was -10 V; the filling pulse was 10 V; and the rate window was $(640\ ms)^{-1}$. For lower doses no defect levels were detected in the DLTS spectra. The defect level $E(250)$ is strongest in the 10^{14} cm^{-2} spectrum.

samples, it is likely that the implant zone, extending ~3.5 μm below the surface, will act as a trap, limiting diffusion of the excitons deeper into the silicon. Since damage centers can be seen in all the samples annealed at 525 °C and in the heavily implanted samples annealed at 750 °C, at least a substantial amount of the PL originates from the implanted region and the PL is monitoring the region of interest in the samples.

For the DLTS data, we expect that when the concentration of a center is lower than about 20% of the background doping, the concentration of a center will very approximately be given by 2 $[P]\Delta C/C$, where $\Delta C/C$ is the fractional change in capacitance and $[P]$ is the concentration of phosphorus donors. In contrast, PL is not usually a quantitative technique, and one must be cautious in comparing data from samples that have different implantation doses; different samples may have different amounts of nonradiative traps and of luminescence traps that are competing for the excitation energy. An estimate of the effects of these other energy channels can be made by again using the PL from the I3 center, with zero-phonon line at 1039.6 meV. All previous work suggests that the I3 center does not involve any impurity in the silicon. The center is easily generated by radiation damage from fast neutrons followed by annealing at ~400 °C, when its strength a in absorption is slightly sublinear in the neutron dose d, $a\sim d^{0.8}$.[21] A very similar exponent of 0.7 has recently been measured using positron annihilation spectroscopy for the vacancy concentration in implanted Si.[22] From Fig. 3 we see that the strength s of the I3 PL line increases with dose d as $s\sim d^{0.7}$ up to 10^{12} cm^{-2}, after which the PL strength declines at 10^{14} cm^{-2}. Then, other very strong PL bands appear (see Fig. 1) that compete with the I3 centers for the available excitation energy. These data demonstrate that up to 10^{12} cm^{-2} the PL strength from a deep center like I3 is closely proportional to its concentration in this sample batch. Over the same dose range, the measured donor and acceptor concentrations are also constant. Consequently, we can interpret the PL strength s of all the lines in the samples implanted at 10^9-10^{12} cm^{-2} as being proportional to their concentration $[C]$, $s\sim c[C]$, although the constant c will be different for each center. The highly nonlinear behavior at low doses of some lines, such as ''M'' and ''T'' in Fig. 3, will be linked in Sec. III C to their containing a minority impurity, carbon. In contrast, lines that increase linearly with dose into the higher dose range (e.g., the 956.5 and 1101.2 meV lines of unknown origin) may be assumed to involve either no impurities or the major impurity in these samples, oxygen.

In this section we have seen that the luminescence is not degraded in spectral quality in any of the samples, and only in the samples annealed at the highest doses does the PL intensity measured in these experiments deviate from being an approximate measure of the concentration of each center. With this information we look next in detail at the DLTS and PL spectra of the annealed samples.

B. Samples annealed at 750 °C

Annealing for 30 min at 750 °C is expected to destroy the simple radiation damage complexes, and the excess self-interstitials are able to diffuse either to the surface or into the bulk of the sample,[23] up to doses at which amorphization occurs. Consistent with this, for annealed samples with relatively low doses of up to 10^{12} cm^{-2}, no DLTS defect levels were detectable, and the PL spectra were indistinguishable from untreated silicon. Only for doses of 10^{13} and 10^{14} cm^{-2} do the DLTS and PL spectra begin to change. In this high dose regime, the DLTS signals $E(110)$, $E(130)$, and $E(250)$ grow (Fig. 4), and closely resemble the spectra recently observed after proton and alpha-particle implanta-

[This article is copyrighted as indicated in the article. Reuse of AIP content is subject to the terms at: http://scitation.aip.org/termsconditions. Downloaded to] IP: 130.56.107.12 On: Fri, 25 Sep 2015 02:34:00

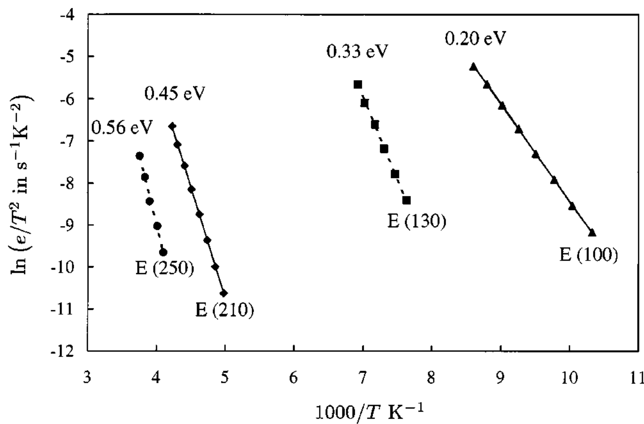

FIG. 5. Arrhenius plots of the electron-emission rate for the defect levels detected in Figs. 4, 9, and 10. The levels with dashed lines are observed after annealing at 750 °C, while the defects with solid lines are observed following thermal treatment at 525 °C.

tion and annealing at 600 °C.[5] The clearly defined $E(130)$ and $E(250)$ traps have energies of $E_c-0.33$ eV, in agreement with Ref. 5, and $E_c-0.56$ eV, respectively (Fig. 5). These data are quantitatively different from the data of Benton *et al.*[13] in which annealing at 750 °C destroyed all the signals; however, those authors noted that several of the defects increased in thermal stability with increasing dose, and our implants, although at the same dose, involved substantially higher beam energies (5.6 MeV compared to 1.2 MeV Si ions). Consequently, the growth in the signal by a factor of 50 [e.g., for $E(130)$] between 10^{13} and 10^{14} cm^{-2} is not necessarily a direct measure of enhanced production, but could indicate increased thermal stability, consistent with Benton *et al.*[13] The $E(130)$ trap at $E_c-0.33$ eV has been identified[5] with the *KA* acceptor center of Benton *et al.* (at $E_c-0.29$ eV), while the $E(250)$ trap at $E_c-0.56$ eV appears to be the *KD* donor defect of Benton *et al.* (at $E_c-0.58$ eV).[5] The dominant feature, the $E(130)$ peak, has been shown to decrease with the production rate of vacancies[5] consistent with the proposal that it is an interstitial cluster.[13] The $E(110)$ peak has only recently been reported;[5] its origin is unknown except that its production in both the present samples and in the *p*-type epi-Si samples of Ref. 5 suggests that impurities are not involved.

The PL spectra of all the samples have many features in common for photon energies greater than ~1030 meV. These transitions, which produce all the PL features in the 10^{12} cm^{-2} sample as shown in Fig. 6, occur through a variety of well-known processes involving exciton recombination.[24] Individual excitons or multi-excitons may recombine at the phosphorus donors or boron acceptors, or they may recombine as free excitons or as an electron-hole plasma. The concentration of isolated P donors can be measured from the intensity of the luminescence emitted by the excitons bound to the donors relative to the free excitons.[25] In all the samples annealed at 750 °C, including those implanted to 10^{13} and 10^{14} cm^{-2}, the concentrations of P and B were invariant by this measure, with random variations of ±15% being ascribed to the material. In Fig. 6, the PL for the high-dose samples shows first, at 10^{13} cm^{-2}, the appear-

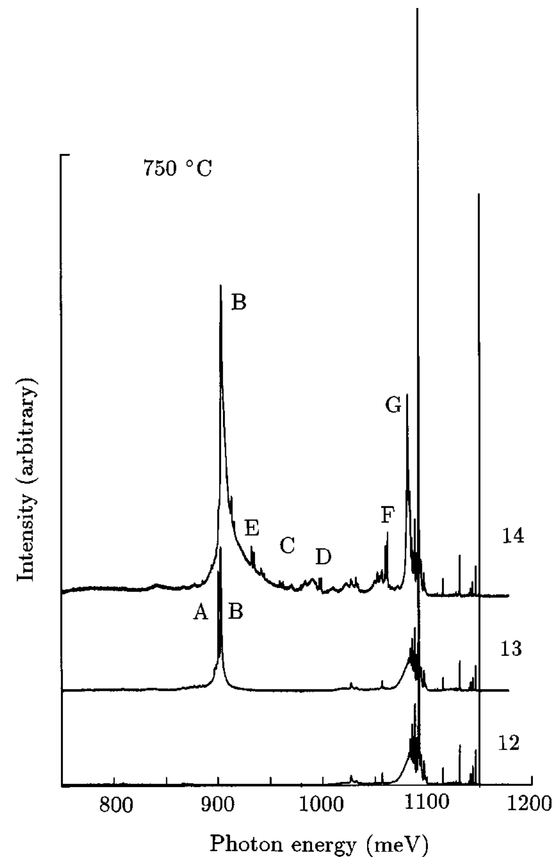

FIG. 6. PL spectra at 4.2 K of samples implanted with 10^{12}–10^{14} cm^{-2} (labeled ''12''–''14'') and annealed at 750 °C. Samples implanted below 10^{12} cm^{-2} gave spectra indistinguishable from the 10^{12} cm^{-2} implant. The features labeled A through G are discussed in the text. PL at energies greater than 1030 meV in the 10^{12} cm^{-2} spectrum (and replicated in the others) is produced by phosphorus, boron, free excitons and the electron-hole plasma. For clarity the spectra are displaced vertically; the zero level is shown by the ends of each spectrum.

ance of sharp lines at 900.0 and 902.4 meV (''*A*'' and ''*B*'' in Fig. 6), and then at 10^{14} cm^{-2} the higher energy component *B* is dominant, together with an asymmetric tail to higher energy: it is now recognizable as the so-called ''903'' line. Using heat treatment alone, it has been found that the 903 line is strongly generated when Czochralski silicon is first heated at ~470 °C to form thermal donors and then heated for a few hours at ~650 °C to release self-interstitials from the donors.[26] The 903 line correlates with {113} defects, which are aggregates of self-interstitials.[27] The origin of this line seems to be a monoclinic *I* center which probably forms part of the self-interstitial aggregate.[26] In the present work, we find that in the 10^{14} cm^{-2} sample, the integrated intensity of the PL from the 903 line decreases by only a factor of ~30 between 4.2 and 240 K (Fig. 7); this remarkable stability is consistent with exciton confinement in the strain field of an aggregate.

Imaging by transmission electron microscopy for the 10^{14} cm^{-2} sample shows that {113} rod-shaped defects are formed, located at a depth of ~3 μm below the wafer surface, near the depth of maximum implant deposition (Fig. 8). Their rod axes are directed along different ⟨110⟩ directions, and they have a very uniform width of ~5 nm. This value is

[This article is copyrighted as indicated in the article. Reuse of AIP content is subject to the terms at: http://scitation.aip.org/termsconditions. Downloaded to] IP: 130.56.107.12 On: Fri, 25 Sep 2015 02:34:00

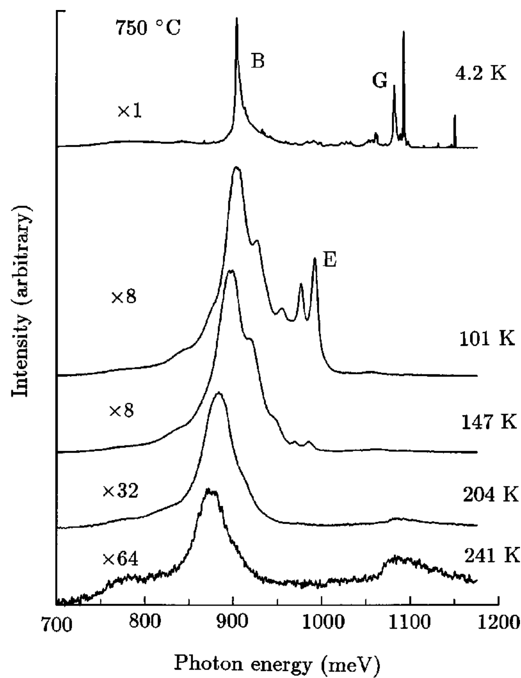

FIG. 7. PL spectra at 4.2–240 K of samples implanted with 10^{14} cm^{-2} and annealed at 750 °C. The intensities have been multiplied by the factors shown for each displayed spectrum. Features ''*B*,'' ''*E*,'' and ''*G*'' are in Fig. 6. Note that with increasing temperature the luminescence towards higher energy is lost first, as the shallower excited states are thermally ionized; the band starting near 1060 meV at 240 K is free-exciton emission. For clarity the spectra are displaced vertically; the zero level is shown by the left end of each spectrum.

in agreement with previous data obtained for different implantation and annealing conditions.[28,29] Their length varies between 88 and 270 nm with an average value of (185 ± 62) nm. Assuming that the number of self-interstitials $n(L)$ condensed into a rod-like defect of length L is $n(L)=\sigma wL$, where w is the width of the defects (taken as 5 nm), and $\sigma=5.5\times10^{14}$ cm^{-2} is the area density of silicon atoms in the {113} defects, the lower bound of the area density N_I of self-interstitials condensed into the {113} defects is estimated as $N_I=(2.3\pm1.6)\times10^{13}$ cm^{-2}, which is comparable to the implanted dose.

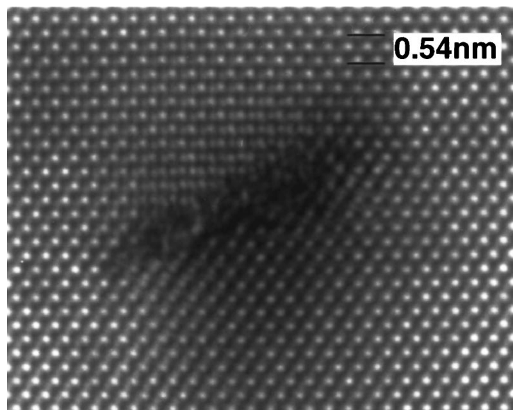

FIG. 8. Transmission electron lattice image of a {113} defect with a width of 5 nm in a sample implanted with 10^{14} cm^{-2} Si ions and annealed at 750 °C.

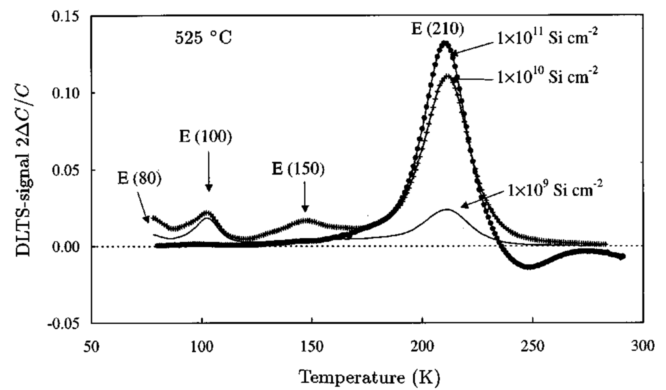

FIG. 9. DLTS spectra of samples implanted with doses from 10^9 to 10^{11} cm^{-2} following a 30 min anneal at 525 °C. The reverse bias was -10 V; the filling pulse was 10 V; and the rate window $(640\ \text{ms})^{-1}$.

The occurrence of the *A* and *B* close pair lines separated by 2.4 meV in the PL spectrum of the 10^{14} cm^{-2} sample is replicated by other defects in the spectrum. Lines with similar separations are seen at 960.2 and 962.2 meV, labeled ''*C*'' in Fig. 6. The lines labeled ''*D*'' at 999.0 and 997.0 meV persist as a dominant feature at high temperature, see Fig. 7. Two other closely paired lines are the ''*E*'' lines at 934.8 and 932.3 meV, and ''*F*'' at 1062.1 and 1060.6 meV. The two lines in each pair do not occur at the same optical center, as judged from the temperature dependence of the lines, and some (the 935 and 1060 meV lines) are detected without their ''partners'' in samples annealed at 525 °C. Finally, one other feature is observed only in the 10^{14} cm^{-2} sample at 1081 meV (''*G*'' on Fig. 6), which has a similar asymmetric shape to the 903 band. None of these features appears to have been reported in the literature. In none of the samples was any significant emission detected using the InSb detector at photon energies between 450 and 750 meV.

We noted in Sec. III A that the widths of the zero-phonon lines are broadened by only 0.3 meV even at the highest dose, 10^{14} cm^{-2}. The exceptions are the 903 and 1081 meV features; the former is believed to be caused by optical sites at self-interstitial aggregates, which are likely to be found in a range of local perturbations. The PL data for the 750 °C anneals are all consistent with the identification of the 903 band as arising from the {113} aggregates;[26] this PL signal can be observed in *n*-type silicon (as here) or in *p*-type silicon (as in Ref. 26). The corresponding dominant DLTS feature in the heavily implanted *n*-type samples is the $E(130)$ level (*KA* in the notation of Ref. 13), which Benton *et al.*[13] have also linked to self-interstitial aggregates; they have also suggested that the same structure produces the $E_v+0.29$ eV and $E_v+0.48$ eV in *p*-type silicon.[30]

C. Samples annealed at 525 °C

The samples annealed at 525 °C show much richer structures with very few damage features in common with the 750 °C set. The DLTS spectra are shown in Figs. 9 and 10, and an overview of the development of the PL spectra has been given in Fig. 1. For clarity, the relative strengths of some of the sharp line features have been presented in Fig. 3, where the strength is defined as the intensity of luminescence

[This article is copyrighted as indicated in the article. Reuse of AIP content is subject to the terms at: http://scitation.aip.org/termsconditions. Downloaded to] IP: 130.56.107.12 On: Fri, 25 Sep 2015 02:34:00

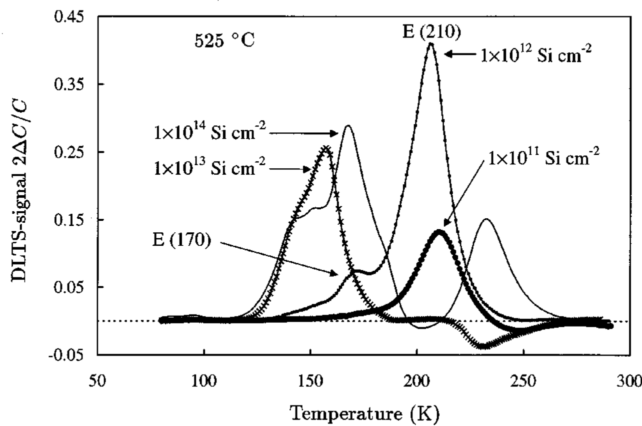

FIG. 10. DLTS spectra of the samples implanted with doses from 10^{11} to 10^{14} cm^{-2} and annealed for 30 min at 525 °C. The reverse bias was -10 V; the filling pulse was 10 V; and the rate window was $(640\ ms)^{-1}$. For doses greater than 10^{12} cm^{-2} the defect concentrations are too high for accurate DLTS measurements with the shallow dopant levels ($\sim 6\times 10^{14}$ cm^{-3}) used here.

integrated over the extent of the spectral feature, with the measurements taken under fixed conditions. PL measurements with the InSb detector show that there is no detectable emission in the range 450–750 meV, except for the most heavily implanted samples (Fig. 11). At 10^{14} cm^{-2}, approximately a quarter of the emission lies below the cutoff of the Ge detector (lower curve of Fig. 11).

Figure 9 shows the evolution of the DLTS spectrum for doses up to 10^{11} cm^{-2} followed by annealing at 525 °C. The

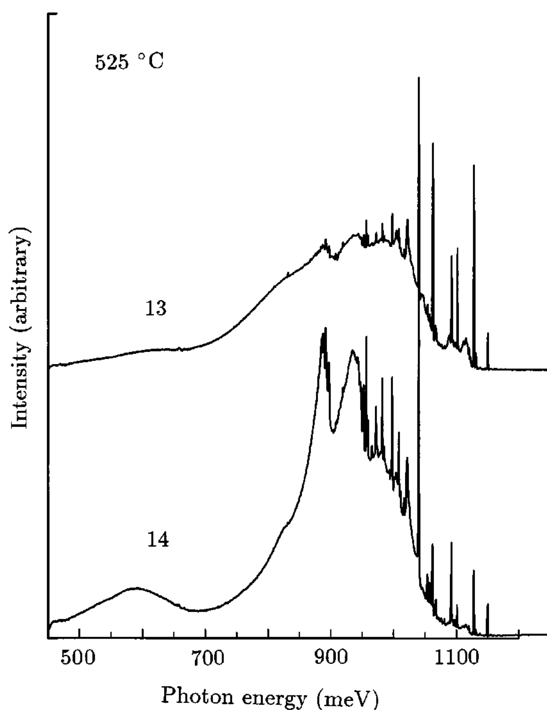

FIG. 11. Extension of the wavelength response to 450 meV in samples implanted with 10^{13} and 10^{14} cm^{-2} and annealed for 30 min at 525 °C shows a continuum of PL at photon energies below the sharp line structure of Fig. 1. Spectra measured at 4.2 K and at a spectral resolution of only ~0.4 meV. For clarity the spectra are displaced vertically; the zero level is shown by the high energy end of each spectrum.

DLTS levels $E(80)$, $E(100)$, and $E(150)$ increase to 10^{10} cm^{-2} and then are not observed at 10^{11} cm^{-2}. Both the ''*M*'' PL line at 761 meV and the *T* PL line at 935 meV also increase and then decrease with dose, well within the range where we have shown in Sec. III A that the PL strength is proportional to the concentration (Figs. 1 and 3). The *T* center is known to be a complex of two carbon atoms and one hydrogen atom,[31] and the *M* center is another *C* and *H* complex;[32] the chemistry of both centers has been determined unambiguously by isotope substitution. The maximum concentration obtained in any given sample will be limited by the concentrations of carbon and also of hydrogen (which may be more significant here since forming the Schottky diode on the DLTS samples is a further processing step compared to the PL samples). The kinetics of producing the *M* and *T* centers are not known, but other carbon-related centers, C_i, C_i-O_i, and C_i-C_s (where *i* denotes an interstitial and *s* a substitutional atom) have been studied as a function of radiation dose. The concentrations of these centers are maximized when the concentration of self-interstitials introduced into the silicon is, within a factor of 2 for all the centers, equal to the initial concentration of C_s. At larger doses, the carbon centers are destroyed as they capture further self-interstitials.[33] The increase and then decrease of the *M* and *T* signals is consistent with this scenario. We identify the $E(100)$ DLTS trap at $E_c-0.20$ eV (see Fig. 5) with the *T* PL center as follows. In the excited state of the *T* transition, an exciton is trapped on the center, resulting in a shallow hole orbiting in the Coulomb field of a deep electron.[31] Taking the binding energy E_b of the effective-mass hole to be $E_b\sim 30$ meV, as is typical for a shallow acceptor, the electron state is located at $E_s=E_g-E_b-E_t$ where E_g is the exciton energy gap (1170 meV), and E_t the transition energy (935 meV), giving $E_s\sim E_c-0.20$ eV. The same energy level argument can be applied to the *M* center, which also has a hole orbiting a tightly bound electron at the center,[32] and it predicts an electron trap level of 0.37 eV. We cannot accurately determine the trap energy of $E(150)$ because of its unresolved structure, but it is estimated to be in the range 0.33–0.38 eV below E_c and so it may be the DLTS analog of the *M* center. The $E(80)$ trap, which also appears only at low doses, is of unknown origin, although it can be distinguished by its rate window from the $E(85)$ hydrogen-related trap of Schmidt *et al.*[5]

With increasing dose the $E(210)$ DLTS center, with its trap level at $E_c-0.45$ eV (Fig. 9), increases in concentration until at a dose of 10^{13} cm^{-2} it is no longer detectable (Figs. 9 and 10). Accurate DLTS spectra are now no longer possible, and the $E(210)$ peak possibly develops into a broadband from extended defects. The only PL feature which is increasing throughout the dose range is the I3 center (Sec. III A). Unfortunately, the excited state of the I3 center[34] cannot be described in the simple way used for the *T* and *M* lines, and we are not able to definitely identify the $E(210)$ center with the I3 center. Although DLTS data becomes less valuable at these doses, PL spectra are still obtainable, and at the highest doses a very large number of optical centers is detected, including two structured bands centered on ~885 and ~930 meV (see Fig. 1) and a considerable amount of

[This article is copyrighted as indicated in the article. Reuse of AIP content is subject to the terms at: http://scitation.aip.org/termsconditions. Downloaded to] IP: 130.56.107.12 On: Fri, 25 Sep 2015 02:34:00

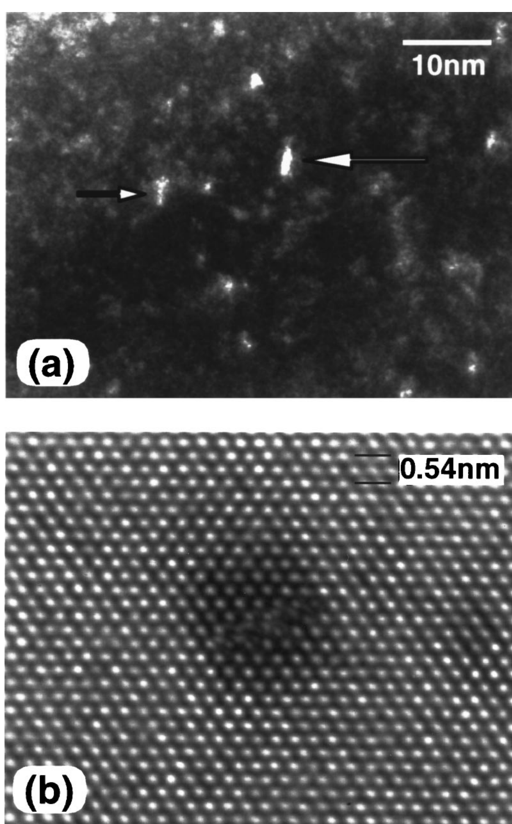

FIG. 12. Transmission electron micrographs of defects in samples implanted with 10^{14} cm^{-2} Si ions and annealed at 525 °C. (a) Weak-beam dark field ($g=\langle 02\bar{2}\rangle$) showing strain contrasts some of which are elongated (arrows) and (b) lattice image showing a defect with a {113} habit plane and a width of 2 nm.

fine structure. In particular, the strongest zero-phonon lines seen at 10^{14} cm^{-2} below the I3 line are at energies of 1008.1, 997.4, 981.7, 972.0, and 956.5 meV. These energies, measured in our ''fully resolved'' spectra, differ significantly from the values quoted in Ref. 12, and the assignments of the lines in that work to known defects (which in fact are not stable at these high annealing temperatures[1]) do not appear to be valid: the lines currently have an unknown origin.

Concurrent with the growth of these multiple lines, isolated strain contrasts at a depth of about 3 μm below the wafer surface are revealed in TEM images, when imaged under weak beam conditions (see Fig. 12). Some of these contrasts appear to be elongated along the projections of Si ⟨110⟩ directions, as shown by the arrows in Fig. 12(a). High-resolution imaging reveals defects with {113} habit planes [see Fig. 11(b)] and a typical width of 2 nm, smaller than the detection limit of ~5 nm used in earlier work.[12,13] The formation of these aggregates after annealing at only 525 °C is significantly lower than the previously reported minimum temperature, 600 °C, for aggregation.[12,13]

IV. SUMMARY

We have examined the DLTS, PL, and TEM signals from *n*-type silicon after implanting with 5.6 MeV Si^{3+} ions using doses of $10^{9}-10^{14}$ cm^{-2} and annealing at 525 and 750 °C. In all the samples, the widths and energies of the PL zero-phonon lines vary little with the treatment, which allows the high resolution of PL to be exploited (Sec. III A).

For samples annealed at 750 °C, line broadening is only significant at the highest doses for two transitions: the 1080 meV PL and for the 903 PL produced by the self-interstitial aggregates of the {113} defect (Sec. III B). The 903 PL is observable in *n*-type or *p*-type silicon, as a result of the ill-defined Fermi energy in PL experiments, and has a possible DLTS counterpart in the $E(130)$ level (*KA* in the notation of Benton *et al.*[13]) in *n*-type silicon and in the B1 and B2 DLTS defects in *p*-type silicon.[30] The PL spectra have allowed us to detect one possible precursor to the {113} defect as the 900 meV line, and the high resolution of PL has established that many previously unreported defects are observed in the 750 °C annealed sample with a dose of 10^{14} cm^{-2} (see Fig. 6). In agreement with Benton *et al.*[13] we find no evidence for loss of *P* or *B* in the implanted layer.

In samples annealed at 525 °C, we have used the high resolving power of PL to unambiguously identify two carbon-hydrogen complexes, and have linked one (the *T* center) to the $E(100)$ DLTS trap at $E_c-0.20$ eV (see Sec. III C). We have shown that over a limited implantation range, $10^{9}-10^{12}$ cm^{-2}, the PL strength can be a measure of the concentration of the centers. Consequently, the loss of the PL signal from the carbon-hydrogen complexes with increasing (but still small) dose has been suggested to be the result of destruction of the centers, paralleling the situation in electron-irradiated silicon where carbon centers act as nucleation points for self-interstitial trapping. One important DLTS signal, $E(120)$ at $E_c-0.45$ eV, and the I3 PL line are observed through a wide range of doses. At the highest doses, new DLTS features and a considerable number of well-resolved but unknown PL defects are created (see Sec. III C). In these samples, TEM imaging shows that nanometer-sized clusters are observable. The modeling of Cowern *et al.*[14] then implies that a range of smaller interstitial clusters exist, which may be the sites of the many PL features. It is evident that photoluminescence studies of the heavily implanted and annealed silicon have the spectral resolution necessary for further studies of the chemistry and structure of the multiplicity of defects.

ACKNOWLEDGMENTS

Financial support by the Swedish Foundation for International Cooperation in Research and Higher Education, the Swedish Research Council for Engineering Sciences, and the EU Commission Contract No. ERBFHRXCT980208 is gratefully acknowledged.

[1] See, e.g., the recent review by B. G. Svensson, *Energy Levels, Structure, and Properties of Point Defects Induced by Ion-Implantation and Electron-Irradiation*, in EMIS data reviews series, ''Properties of Silicon,'' (The Institution of Electrical Engineers, London), p. 763.

[2] For a recent review, see K. S. Jones, *Structure of Ion-Implantation Induced Defects in c-Si*, in EMIS data reviews series, ''Properties of Silicon,'' (The Institution of Electrical Engineers, London), p. 755.

[3] D. C. Schmidt, B. G. Svensson, S. Godey, E. Ntsoenzok, J. F. Barbot, and C. Blanchard, Nucl. Instrum. Methods Phys. Res. B **147**, 106 (1998).

[4] V. V. Bolotov, V. M. Emeksuzyan, G. L. Plotnikov, and E. N. Vologdin, Nucl. Instrum. Methods Phys. Res. B **80/81**, 667 (1993).

[This article is copyrighted as indicated in the article. Reuse of AIP content is subject to the terms at: http://scitation.aip.org/termsconditions. Downloaded to] IP: 130.56.107.12 On: Fri, 25 Sep 2015 02:34:00

[5] D. C. Schmidt, B. G. Svensson, J. F. Barbot, and C. Blanchard, Nucl. Instrum. Methods Phys. Res. B **155**, 60 (1999).
[6] Yu. R. Suprun-Belevich and L. Palmetshofer, Nucl. Instrum. Methods Phys. Res. B **96**, 245 (1995).
[7] Yu. Suprun-Belevich, L. Palmetshofer, B. J. Sealy, and N. Emerson, Semicond. Sci. Technol. **14**, 565 (1999).
[8] N. M. Johnson, D. J. Bartelink, R. B. Gold, and J. F. Gibbons, J. Appl. Phys. **50**, 4828 (1979).
[9] S. Fatima, J. Wong-Leung, J. Fitz Gerald, and C. Jagadish, Appl. Phys. Lett. **72**, 3044 (1998).
[10] S. Fatima, J. Wong-Leung, J. Fitz Gerald, and C. Jagadish, Appl. Phys. Lett. **74**, 1141 (1999).
[11] K. Terashima, T. Ikarashi, M. Watanabe, and T. Kitano, Mater. Sci. Forum **258–263**, 587 (1997).
[12] S. Coffa, S. Libertino, and C. Spinella, Appl. Phys. Lett. **76**, 321 (2000).
[13] J. L. Benton, K. Halliburton, S. Libertino, D. J. Eaglesham, and S. Coffa, J. Appl. Phys. **84**, 4749 (1998).
[14] N. E. B. Cowern, G. Mannino, P. A. Stolk, F. Roozeboom, H. G. A. Huizing, J. G. M. van Berkum, F. Christiano, A. Claverie, and M. Jaraíz, Phys. Rev. Lett. **82**, 4460 (1999).
[15] J. F. Ziegler, J. P. Biersack, and U. Littmark, *The Stopping and Range of Ions in Solids* (Pergamon, New York, 1985), Vol. 1; for further information and download see also http://www.research.ibm.com/ionbeams/home.htm.
[16] B. G. Svensson, K.-H. Rydn, and B. M. S. Lewerentz, J. Appl. Phys. **66**, 1699 (1989).
[17] G. Davies, Phys. Rep. **176**, 83 (1989).
[18] For example, A. M. Stoneham, Proc. Phys. Soc. **89**, 909 (1966) predicts that the linewidth is proportional to the square root of the dislocation density when macroscopic defects such as dislocations are significant.
[19] E. C. Lightowlers, V. Higgs, M. J. Gregson, G. Davies, S. T. Davey, C. J. Gibbings, C. G. Tuppen, F. Schäffler, and E. Kasper, Thin Solid Films **183**, 235 (1989).
[20] N. de Mello, G. Davies, E. C. Lightowlers, and V. Higgs, Thin Solid Films **183**, 273 (1989).
[21] G. Davies, E. C. Lightowlers, and Z. E. Ciechanowska, J. Phys. C **20**, 191 (1987).
[22] A. P. Knights, F. Malik, and P. G. Coleman, Appl. Phys. Lett. **75**, 466 (1999).
[23] See, e.g., J. D. Plummer, Mater. Res. Soc. Symp. Proc. **469**, 3 (1997).
[24] M. L. W. Thewalt, in *Excitons*, edited by E. I. Rashba and M. D. Sturge (North-Holland, Amsterdam, 1982), p. 393.
[25] P. McL. Colley and E. C. Lightowlers, Semicond. Sci. Technol. **2**, 157 (1987).
[26] E. C. Lightowlers, L. Jeyanathan, A. N. Safonov, V. Higgs, and G. Davies, Mater. Sci. Eng., B **24**, 144 (1994).
[27] S. Takeda, S. Muto, and M. Hirata, Mater. Sci. Forum **83–87**, 309 (1992).
[28] M. Seibt, J. Imschweiler, and H.-A. Hefner, in *Semiconductor Silicon 1994*, edited by H. R. Huff, W. Bergholz, and K. Sumino (The Electrochemical Society, Pennington, NJ, 1994), p. 720.
[29] D. A. Eaglesham, P. A. Stolk, H.-J. Gossmann, and J. M. Poate, Appl. Phys. Lett. **65**, 2305 (1994).
[30] J. L. Benton, S. Libertino, P. Kringhoj, D. J. Eaglesham, J. M. Poate, and S. Coffa, J. Appl. Phys. **82**, 120 (1997).
[31] A. N. Safonov, E. C. Lightowlers, G. Davies, P. Leary, R. Jones, and S. Öberg, Phys. Rev. Lett. **77**, 4812 (1996).
[32] A. N. Safonov, E. C. Lightowlers, and G. Davies, *Proceedings of the International Conference on Physics of Semiconductors*, edited by D. J. Lockwood, Vancouver (World Scientific, Singapore, 1994), Vol. 3, p. 2239.
[33] G. Davies and R. C. Newman, Carbon in monocrystalline silicon, in *Handbook on Semiconductors*, edited by T. S. Moss (Elsevier, New York, 1994), pp. 1557–1635.
[34] Z. E. Ciechanowska, G. Davies, and E. C. Lightowlers, Solid State Commun. **49**, 427 (1984).

[This article is copyrighted as indicated in the article. Reuse of AIP content is subject to the terms at: http://scitation.aip.org/termsconditions. Downloaded to] IP: 130.56.107.12 On: Fri, 25 Sep 2015 02:34:00